

Gapped Spin-1/2 Spinon Excitations in a New Kagome Quantum Spin Liquid Compound $\text{Cu}_3\text{Zn}(\text{OH})_6\text{FBr}$ *

Zili Feng(冯子力)^{1†}, Zheng Li(李政)^{1,2†}, Xin Meng(孟鑫)¹, Wei Yi(衣玮)¹, Yuan Wei(魏源)¹, Jun Zhang(张骏)³, Yan-Cheng Wang(王艳成)¹, Wei Jiang(蒋伟)⁴, Zheng Liu(刘峥)⁵, Shiyan Li(李世燕)^{3,6}, Feng Liu(刘锋)⁴, Jianlin Luo(雒建林)^{1,2,7}, Shiliang Li(李世亮)^{1,2,7}, Guo-qing Zheng(郑国庆)^{1,8**}, Zi Yang Meng(孟子杨)^{1**}, Jia-Wei Mei(梅佳伟)^{9,4,10**}, Youguo Shi(石友国)^{1**}

¹Institute of Physics, Chinese Academy of Sciences, Beijing 100190

²School of Physical Sciences, University of Chinese Academy of Sciences, Beijing 100190

³State Key Laboratory of Surface Physics, Department of Physics, and Laboratory of Advanced Materials, Fudan University, Shanghai 200433

⁴Department of Materials Science and Engineering, University of Utah, Salt Lake City, Utah 84112, USA

⁵Institute for Advanced Study, Tsinghua University, Beijing 100084

⁶Collaborative Innovation Center of Advanced Microstructures, Nanjing 210093

⁷Collaborative Innovation Center of Quantum Matter, Beijing 100190

⁸Department of Physics, Okayama University, Okayama 700-8530, Japan

⁹Institute for Quantum Science and Engineering, and Department of Physics, Southern University of Science and Technology, Shenzhen 518055

¹⁰Beijing Computational Science Research Center, Beijing 100193

(Received 15 June 2017)

We report a new kagome quantum spin liquid candidate $\text{Cu}_3\text{Zn}(\text{OH})_6\text{FBr}$, which does not experience any phase transition down to 50 mK, more than three orders lower than the antiferromagnetic Curie-Weiss temperature (~ 200 K). A clear gap opening at low temperature is observed in the uniform spin susceptibility obtained from ^{19}F nuclear magnetic resonance measurements. We observe the characteristic magnetic field dependence of the gap as expected for fractionalized spin-1/2 spinon excitations. Our experimental results provide firm evidence for spin fractionalization in a topologically ordered spin system, resembling charge fractionalization in the fractional quantum Hall state.

PACS: 75.10.Kt, 67.30.er, 05.30.Pr, 75.40.Cx

DOI: 10.1088/0256-307X/34/7/077502

When subject to strong geometric frustrations, quantum spin systems may achieve paramagnetic ground states dubbed quantum spin liquid (QSL).^[1] It is characterized by the pattern of long-range quantum entanglement that has no classical counterpart.^[2–4] QSL is an unambiguous Mott insulator whose charge gap is not associated with any symmetry breaking.^[1] It is related to the mechanism of high-temperature superconductivity^[1] and the implementation of topological quantum computation.^[5] The underlying principle of QSL, i.e. topological orders due to quantum entanglement,^[3,4] is beyond the Landau symmetry-breaking paradigm^[2] and has been realized in fractional quantum Hall systems,^[6] resulting in fractionalized $e/3$ charged anyon.^[7,8] Similarly, fractionalized spin-1/2 spinon excitations are allowed in QSL.^[9–12]

Kagome Heisenberg antiferromagnets are promis-

ing systems for the pursuit of QSL.^[13–15] For example, herbertsmithite $\text{ZnCu}_3(\text{OH})_6\text{Cl}_2$ is a famous kagome system, which displays a number of well-established QSL behaviors.^[16–29] Inelastic neutron scattering measurements have detected continuum of spin excitations^[25] while nuclear magnetic resonance (NMR) measurements suggest a finite gap at low temperature.^[29] However, multiple NMR lines of nuclear spins with $I > 1/2$ can not be easily resolved, particularly in the presence of residual interkagome Cu^{2+} spin moments even in high-quality single crystals.^[20,23,28,29] Furthermore, although it is commonly accepted that the quantum number of spinons is spin-1/2, no direct evidence has been observed.^[29] Therefore, it is crucial to find new QSL systems to unambiguously demonstrate the spin-1/2 quantum number of spinons.

*Supported by the National Key Research and Development Program of China under Grant Nos 2016YFA0300502, 2016YFA0300503, 2016YFA0300604, 2016YF0300300 and 2016YFA0300802, the National Natural Science Foundation of China under Grant Nos 11421092, 11474330, 11574359, 11674406, 11374346 and 11674375, the National Basic Research Program of China (973 Program) under Grant No 2015CB921304, the National Thousand-Young-Talents Program of China, the Strategic Priority Research Program (B) of the Chinese Academy of Sciences under Grant Nos XDB07020000, XDB07020200 and XDB07020300. The work in Utah is supported by DOE-BES under Grant No DE-FG02-04ER46148.

†These two authors contributed to this work equally.

**Corresponding author. Email: gqzheng@iphy.ac.cn; zymeng@iphy.ac.cn; jiawei.mei@gmail.com; ygshi@iphy.ac.cn

© 2017 Chinese Physical Society and IOP Publishing Ltd

Recently, barlowite $\text{Cu}_4(\text{OH})_6\text{FBr}$ has attracted much attention as a new kagome system with minimum disorder.^[30–35] As opposed to herbertsmithite with *ABC*-stacked kagome planes, barlowite crystallizes in high-symmetry hexagonal rods owing to direct *AA* kagome stacking. It has also been found that the in-plane Dzyaloshinskii-Moriya interaction in barlowite is an order of magnitude smaller than that

in herbertsmithite.^[35] Consequently, the QSL physics has been suggested to be present at relative high temperature. Unfortunately, the material goes through an antiferromagnetic transition at ~ 15 K.^[32,35] It has thus been proposed that substituting the interkagome Cu^{2+} sites with non-magnetic ions may suppress the magnetic transition and ultimately lead to a QSL ground state.^[15,32,34,36]

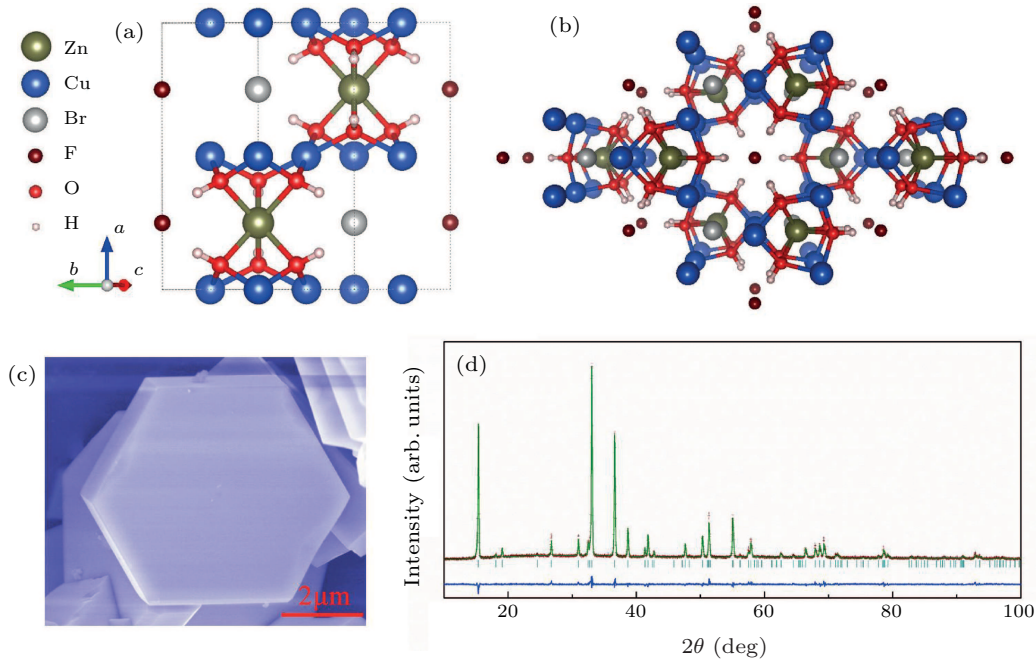


Fig. 1. (a) Schematic crystal structure of $\text{Cu}_3\text{Zn}(\text{OH})_6\text{FBr}$ with copper Cu^{2+} ions (blue) forming the kagome planes *AA* stacked along *c*-axis. Kagome planes are separated by non-magnetic Zn^{2+} (blond) ions. (b) Top view of the $\text{Cu}_3\text{Zn}(\text{OH})_6\text{FBr}$ crystal structure, where F (brown) is in the center between two hexagons of two kagome Cu planes. (c) Scanning electron microscope image of crystal grain in the polycrystalline samples. (d) Measured (brown +) and calculated (green line) XRD diffraction intensities of polycrystalline samples. The blue curve indicates the difference between the measured and calculated intensities. The vertical lines indicate peak positions.

Table 1. Structure parameters of $\text{Cu}_3\text{Zn}(\text{OH})_6\text{FBr}$ at room temperature. Space group $P6_3/mmc$; $a = b = 6.6678(2)$ Å, $c = 9.3079(3)$ Å.

Site	<i>w</i>	<i>x</i>	<i>y</i>	<i>z</i>	<i>B</i> (Å ²)
Cu	6 <i>g</i>	0.5	0	0	1.48(6)
Zn	2 <i>d</i>	1/3	2/3	3/4	1.93(8)
Br	2 <i>c</i>	2/3	1/3	3/4	1.99(5)
F	4 <i>b</i>	0.0	0.0	3/4	0.34(2)
O	12 <i>k</i>	0.1887	0.8113(5)	0.9021(7)	2.22(2)
H	12 <i>k</i>	0.1225	0.8775	0.871	1.0

In this Letter, we report a new kagome QSL candidate $\text{Cu}_3\text{Zn}(\text{OH})_6\text{FBr}$. It does not experience any phase transition down to 50 mK, more than three orders lower than the antiferromagnetic Curie-Weiss temperature (~ 200 K). ^{19}F NMR measurements reveal a gapped QSL ground state in $\text{Cu}_3\text{Zn}(\text{OH})_6\text{FBr}$. The field dependence of the gap implies a zero-field gap 7.5 ± 0.4 K and spin-1/2 quantum number for spin excitations, i.e. spinons.

We have successfully synthesized $\text{Cu}_3\text{Zn}(\text{OH})_6\text{FBr}$

polycrystalline samples by replacing the interkagome Cu^{2+} sites in $\text{Cu}_4(\text{OH})_6\text{FBr}$ with non-magnetic Zn^{2+} . Our thermodynamical (e.g. magnetic susceptibility and specific heat) measurements were carried out on the Physical Properties Measurement Systems (PPMS). The NMR spectra of ^{19}F with the nuclear gyromagnetic ratio $\gamma = 40.055$ MHz/T were obtained by integrating the spin echo as a function of the RF frequency at constant external magnetic fields of 0.914 T, 3 T, 5.026 T and 7.864 T, respectively.

Figures 1(a) and 1(b) depict the crystal structure of $\text{Cu}_3\text{Zn}(\text{OH})_6\text{FBr}$. Micrometer-size crystals are easily observed by the scanning electron microscope (SEM) (Fig. 1(c)). The refinement of the powder x-ray diffraction pattern (Fig. 1(d)) shows that the material crystallizes in $P6_3/mmc$ space group with Cu^{2+} ions forming a direct stack of undistorted kagome planes separated by non-magnetic Zn^{2+} ions (Figs. 1(a) and (b)) as expected from theoretical

calculations.^[34] $\text{Cu}_3\text{Zn}(\text{OH})_6\text{FBr}$ is a charge-transfer insulator and the charge gap between $\text{Cu-}3d^9$ and $\text{O-}2p$ orbitals is around 1.8 eV according to first principles calculations.^[34,37] Powder x-ray diffraction measurements were carried out using $\text{Cu } K_\alpha$ radiation at room temperature. The diffraction data is analyzed by the Rietveld method using the program RIETAN-FP.^[38] All positions are refined as fully occupied with the initial atomic positions taken from $\text{Cu}_4(\text{OH})_6\text{FBr}$.^[31] The refined results are summarized in Table 1.

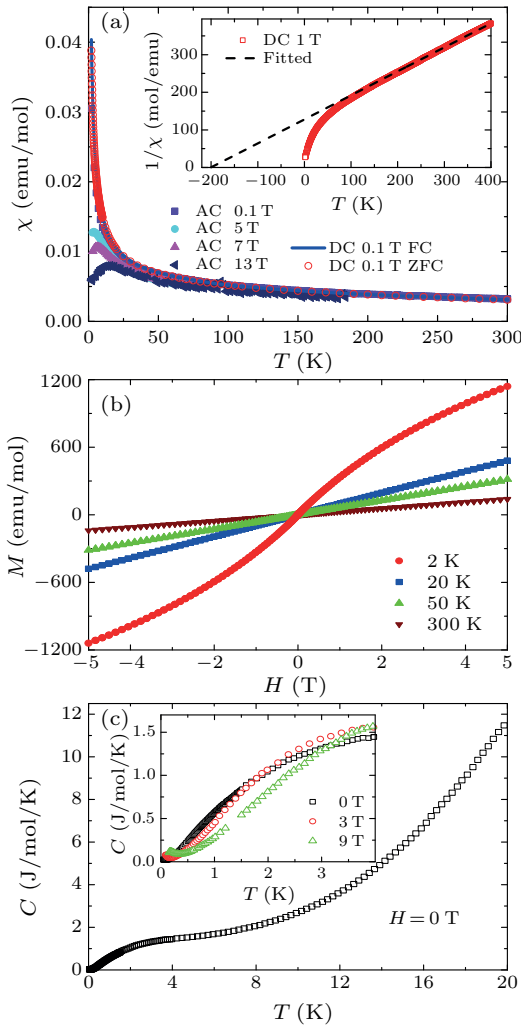


Fig. 2. (a) Temperature dependence of magnetic susceptibility under different magnetic fields measured by both DC and AC methods. In AC measurements, the oscillation field amplitude is 17 Oe and the oscillation frequency is 633 Hz. The inset shows the temperature dependence of the inverse susceptibility $1/\chi$ at 1 T. (b) Magnetic field dependence of magnetization at different temperatures. (c) Temperature dependence of the specific heat at zero field down to 50 mK. The inset shows the magnetic field effect on the specific heat at low temperatures.

No phase transition is observed in our thermodynamical measurements (Fig. 2), establishing strong evidence for a QSL ground state in $\text{Cu}_3\text{Zn}(\text{OH})_6\text{FBr}$. Temperature dependence of magnetic susceptibility

under different magnetic fields does not display any magnetic transition down to 2 K as shown in Fig. 2(a). No splitting is detected between the field-cooled (FC) and zero-field-cooled (ZFC) results down to 2 K, indicating the absence of spin glass transition. At high temperature, magnetic susceptibility can be well fitted by the Curie-Weiss law with the Curie temperature and Curie constant as -200 K and 1.57 K \cdot emu/mol, respectively. This indicates a strong antiferromagnetic superexchange interaction $J \sim 17$ meV among Cu^{2+} moments in the kagome planes. The g -factor is estimated to be about $g = 2.4$, consistent with the g -factor measurements in the Barlowite.^[35] In Fig. 2(b), no visible hysteresis loop is observed in the magnetic field dependence of magnetization at different temperatures. Figure 2(c) is the specific heat measurement at zero field down to 50 mK. The inset shows the magnetic field effect on the specific heat at low temperatures, which exhibits upturn behavior at high field due to nuclear Schottky anomaly.

There are residual interkagome Cu^{2+} (RIC) moments due to incomplete Zn^{2+} substitution in $\text{Cu}_3\text{Zn}(\text{OH})_6\text{FBr}$. Few Zn^{2+} exists in kagome planes according to the line shape of NMR spectra (see below for Fig. 3). The energy dispersive x-ray spectroscopy measurements at different locations indicate that the composition is stoichiometric with the atomic ratio between Cu and Zn as 1:0.36. The inductively coupled plasma atomic emission spectroscopy analysis suggests the atomic ratio between Cu and Zn as 1:0.30. From the chemical component analysis, we roughly estimate the concentration of the RIC moments to be $\sim 10\%$, comparable to those in herbertsmithite.^[39]

At low temperatures, RIC moments obscure the intrinsic kagome plane QSL behaviors in the bulk magnetic susceptibility and heat capacity, similar to previous results of herbertsmithite.^[22,39–43] DC susceptibility at low temperatures in 0.1 T magnetic field is fitted by Curie-Weiss behavior with Curie constant and Curie temperature as 0.18 K \cdot emu/mol and -2.9 K, respectively, indicating weak antiferromagnetically interacting RIC moments. Under high magnetic fields, the RIC moments freeze and the AC susceptibility drops at low temperatures (see Fig. 2(a)). We also measure T -dependent AC susceptibilities for various frequencies and magnetic fields at low temperatures, see Fig. S7 in the supplementary materials (SM).^[44] The AC susceptibility is independent of frequencies, implying that RIC moments do not develop spin glass freezing down to 2 K. The RIC moments also contribute a shoulder in the specific heat measurements at low temperatures (see Fig. 2(c)). The shoulder is suppressed in magnetic fields, as shown in the inset of Fig. 2(c), along which the RIC moments are polarized, similar to herbertsmithite.^[41]

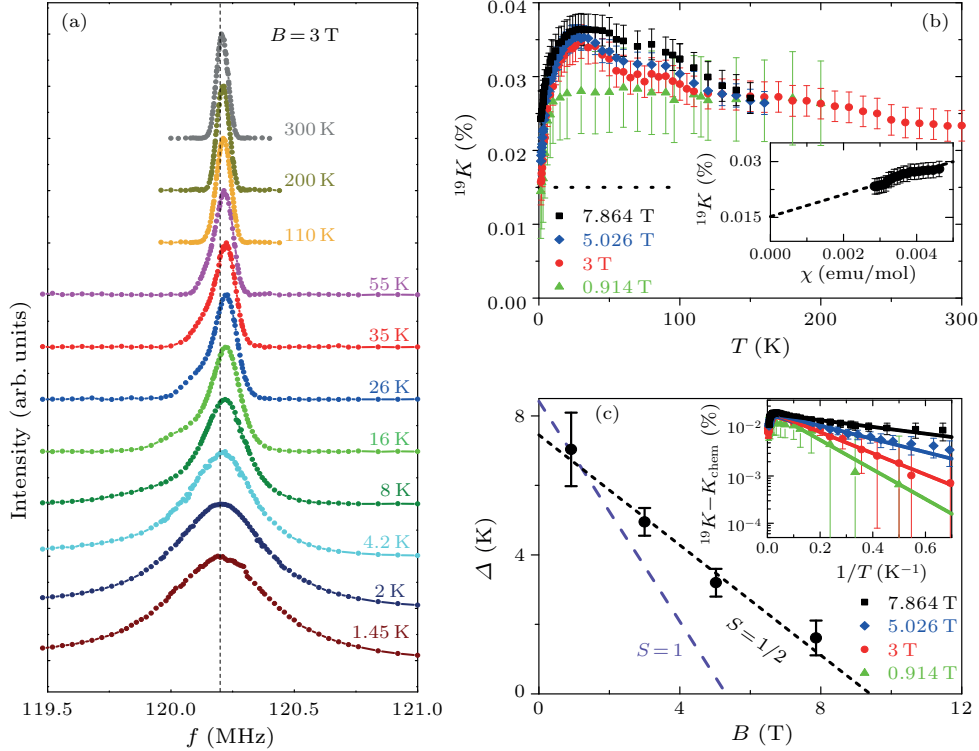


Fig. 3. (a) ^{19}F NMR spectra under 3 T at different temperatures. The vertical dash line $f_0 = 120.199$ MHz, corresponding to the chemical shift, is a guide to the eyes. (b) Temperature dependence of the Knight shift ^{19}K determined from the peak positions of the spectra. The dotted horizontal line shows the position of K_{chem} obtained from the $^{19}\text{K}-\chi$ plot at high temperatures as shown in the inset. (c) Magnetic field dependence of the spin gap. The black short-dash line is fitted by $\Delta(B) = \Delta(0) - g\mu_{\text{B}}SB$ with spin quantum number $S = 1/2$. For comparison, we also plot $\Delta(B)$ for $S = 1$ shown by the blue dash line constrained by the value at 0.914 T, which hardly describes the data. The inset shows the Arrhenius plot of $^{19}\text{K} - K_{\text{chem}}$ with the vertical axis in logarithmic scale, which demonstrates visually that the gap decreases with increasing magnetic field. The solid curve is the fitting function $A \exp(-\Delta/T)$ for $^{19}\text{K} - K_{\text{chem}}$.

To directly unveil QSL physics in kagome plane, we implement NMR measurements to probe uniform spin susceptibility of kagome Cu^{2+} spin moments in $\text{Cu}_3\text{Zn}(\text{OH})_6\text{FBr}$. A unique advantage of $\text{Cu}_3\text{Zn}(\text{OH})_6\text{FBr}$ for the NMR measurements is that it contains ^{19}F . It is known that ^{2}D , ^{17}O and ^{35}Cl NMR measurements in herbertsmithite are rather difficult due to multiple resonance peaks resulted from nuclear spins $I = 1$, $I = 5/2$ and $I = 3/2$, respectively.^[20,23,28,29] In contrast, only one resonance peak needs to be resolved for ^{19}F with $I = 1/2$ nuclear spin, as shown in Fig. 3(a). The sharp high-temperature peaks suggest that few ions of Zn^{2+} exist in kagome planes. Moreover, no extra peak due to RIC moments is observed even at low temperatures. The line shape asymmetry may arise from the magnetic anisotropy, e.g. $g_{\parallel}/g_{\perp} = 2.42/2.21$ in Barlowite.^[35] We have also carried out the measurements with different pulse interval (τ) in NMR echo to exclude the possibility of impurity moment contributions in the NMR spectrum.^[44]

In a gapped QSL, the spin susceptibility should become zero at low temperature. The Knight shift is related to the uniform susceptibility χ as $^{19}\text{K} = A_{\text{hf}}\chi +$

K_{chem} , where A_{hf} is the hyperfine coupling constant between the ^{19}F nuclear spin and the electron spins, and K_{chem} is the T -independent chemical shift. $K_{\text{chem}} = 0.015\%$ is obtained from the $^{19}\text{K}-\chi$ plot at high temperatures as shown in the inset of Fig. 3(b), where χ is the DC susceptibility at $B = 3$ T. Figure 3(b) shows that the Knight shift drops quickly below ~ 30 K. At high temperatures (~ 100 K), the Knight shift ^{19}K has a systematic variation as a function of magnetic field, whose origin is unclear at present and left for future investigation, but we note that such a behavior would not change our results at low temperatures below 30 K. The Knight shift at low fields (0.914 T and 3 T) tends to merge to K_{chem} at low temperatures, similar to the previous results of herbertsmithite.^[29] The inset of Fig. 3(c) is the Arrhenius plot of $^{19}\text{K} - K_{\text{chem}}$, where the low-temperature data can be well fitted by an exponential function $A \exp(-\Delta/T)$, with A and Δ as fitting parameters for a constant and the gap value, respectively. In the fit, we fixed $K_{\text{chem}} = 0.015\%$.

With elevating the magnetic fields, the gap is suppressed due to Zeeman effect as $\Delta(B) = \Delta(0) - g\mu_{\text{B}}SB$, where μ_{B} is Bohr magneton. From the linear

fitting of the field dependence of Δ , we obtain a zero-field gap 7.5 ± 0.4 K and $gS = 1.16 \pm 0.11$. Regarding to $g = 2.4$ obtained from bulk magnetic susceptibility measurements in Fig. 2(a), $gS = 1.16 \pm 0.11$ confirms a spin quantum number $S = 1/2$ and $g = 2.32 \pm 0.22$. The spin $S = 1/2$ quantum number implies fractionalized spinon excitations in the quantum spin liquid compound $\text{Cu}_3\text{Zn}(\text{OH})_6\text{FBr}$.

Detecting the spin-1/2 quantum number of spin excitations in a QSL state is of great significance. Spin-1/2 spinon excitations have been discussed since the early stage of spin liquid theory,^[9] yet there is no direct experimental confirmation of the spin-1/2 quantum number till now. Our results show that $\text{Cu}_3\text{Zn}(\text{OH})_6\text{FBr}$ has a gapped QSL ground state, consistent with the results in herbertsmithite,^[29] and unambiguously manifest the spin-1/2 quantum number of spinons. It reflects the spin fractionalization in a QSL state when spin rotation symmetry meets topology. Within minimal symmetry (e.g. time reversal symmetry and translational symmetry) assumptions, a gapped kagome QSL should be \mathbb{Z}_2 -gauge type^[11,12] (i.e. toric code type^[5]) according to the theoretical constraints.^[45]

In conclusion, we have successfully synthesized a new kagome compound $\text{Cu}_3\text{Zn}(\text{OH})_6\text{FBr}$ and its quantum spin liquid ground state is verified in our thermodynamical measurements. Our ^{19}F NMR data reveals a gapped spin-liquid ground state for $\text{Cu}_3\text{Zn}(\text{OH})_6\text{FBr}$, similar to previous ^{17}O NMR results on herbertsmithite. Most importantly, we provide experimental evidence for spin-1/2 quantum number for spin excitations, i.e. spinons. We therefore believe that $\text{Cu}_3\text{Zn}(\text{OH})_6\text{FBr}$ provides a promising platform for future investigations of the topological properties of quantum spin liquid states.

We acknowledge Yongqing Li for discussions on the magnetic susceptibility measurements. We thank Xi Dai and Zhong Fang for useful discussions.

References

- [1] Anderson P W 1987 *Science* **235** 1196
- [2] Wen X 2004 *Quantum Field Theory of Many-Body Systems: From the Origin of Sound to an Origin of Light and Electrons* Oxford Graduate Texts (OUP Oxford, 2004)
- [3] Kitaev A and Preskill J 2006 *Phys. Rev. Lett.* **96** 110404
- [4] Levin M and Wen G 2006 *Phys. Rev. Lett.* **96** 110405
- [5] Kitaev A Y 2003 *Ann. Phys. (N. Y.)* **303** 2
- [6] Tsui D C, Stormer H L and Gossard A C 1982 *Phys. Rev. Lett.* **48** 1559
- [7] Laughlin R B 1983 *Phys. Rev. Lett.* **50** 1395
- [8] R de Picciotto, Reznikov M, Heiblum M, Umansky V, Bunin G and Mahalu D 1997 *Nature* **389** 162
- [9] Kivelson S A, Rokhsar D S and Sethna J P 1987 *Phys. Rev. B* **35** 8865
- [10] Read N and Chakraborty B 1989 *Phys. Rev. B* **40** 7133
- [11] Read N and Sachdev S 1991 *Phys. Rev. Lett.* **66** 1773
- [12] Wen X G 1991 *Phys. Rev. B* **44** 2664
- [13] Lee P A 2008 *Science* **321** 1306
- [14] Balents L 2010 *Nature* **464** 199
- [15] Norman M R 2016 *Rev. Mod. Phys.* **88** 041002
- [16] Shores M P, Nytko E A, Bartlett B M and Nocera D G 2005 *J. Am. Chem. Soc.* **127** 13462
- [17] Helton J S, Matan K, Shores M P, Nytko E A, Bartlett B M, Yoshida Y, Takano Y, Suslov A, Qiu Y, Chung H, Nocera D G and Lee Y S 2007 *Phys. Rev. Lett.* **98** 107204
- [18] Mendels P, Bert F, M A de Vries, Olariu A, Harrison A, Duc F, Trombe J C, Lord J S, Amato A and Baines C 2007 *Phys. Rev. Lett.* **98** 077204
- [19] Zorko A, Nellutla S, J van Tol, Brunel L C, Bert F, Duc F, Trombe C, M A de Vries, Harrison A and Mendels P 2008 *Phys. Rev. Lett.* **101** 026405
- [20] Imai T, Nytko E A, Bartlett B M, Shores M P and Nocera D G 2008 *Phys. Rev. Lett.* **100** 077203
- [21] M A de Vries, Stewart J R, Deen P P, Piatek J O, Nilsen G J, H M Rønnow and Harrison A 2009 *Phys. Rev. Lett.* **103** 237201
- [22] Helton J S, Matan K, Shores M P, Nytko E A, Bartlett B M, Qiu Y, Nocera D G and Lee Y S 2010 *Phys. Rev. Lett.* **104** 147201
- [23] Imai T, Fu M, Han T H and Lee Y S 2011 *Phys. Rev. B* **84** 020411
- [24] Jeong M, Bert F, Mendels P, Duc F, Trombe J C, M A de Vries and Harrison A 2011 *Phys. Rev. Lett.* **107** 237201
- [25] Han T H, Helton J S, Chu S, Nocera D G, Rodriguez-Rivera J A, Broholm C and Lee Y S 2012 *Nature* **492** 406
- [26] Han T H, Chu S and Lee Y S 2012 *Phys. Rev. Lett.* **108** 157202
- [27] Han T H, Helton J S, Chu S, Prodi A, Singh D K, Mazzoli C, Müller P, Nocera D G and Lee Y S 2011 *Phys. Rev. B* **83** 100402
- [28] Olariu A, Mendels P, Bert F, Duc F, Trombe J C, de Vrie M As and Harrison A 2008 *Phys. Rev. Lett.* **100** 087202
- [29] Fu M, Imai T, Han T H and Lee Y S 2015 *Science* **350** 655
- [30] Elliot P and Cooper M 2010 *Mineral. Mag.* **74** 797
- [31] Elliot P, Cooper M and Pring A 2014 *Mineral. Mag.* **78** 1755
- [32] Han T H, Singleton J and Schlueter J A 2014 *Phys. Rev. Lett.* **113** 227203
- [33] Jeschke H O, Salvat-Pujol F, Gati E, Hoang N H, Wolf B, Lang M, Schlueter J A and Valentí R 2015 *Phys. Rev. B* **92** 094417
- [34] Liu Z, Zou X, Mei J W and Liu F 2015 *Phys. Rev. B* **92** 220102
- [35] Han T H, Isaacs E D, Schlueter J A and Singleton J 2016 *Phys. Rev. B* **93** 214416
- [36] Guterding D, Valentí R and Jeschke H O 2016 *Phys. Rev. B* **94** 125136
- [37] Liu Z, Mei J W and Liu F 2015 *Phys. Rev. B* **92** 165101
- [38] Rietveld H M 1969 *J. Appl. Crystallogr.* **2** 65
- [39] Freedman D E, Han T H, Prodi A, Müller P, Huang Z, Chen S, Webb S M, Lee Y S, McQueen T M and Nocera D G 2010 *J. Am. Chem. Soc.* **132** 16185
- [40] Bert F, Nakamae S, Ladiou F, L'Hôte D, Bonville P, Duc F, Trombe C and Mendels P 2007 *Phys. Rev. B* **76** 132411
- [41] Vries M A de, Kamenev K V, Kockelmann W A, Sanchez-Benitez J and Harrison A 2008 *Phys. Rev. Lett.* **100** 157205
- [42] Han T H, Norman M R, Wen J, Rodriguez-Rivera J A, Helton J S, Broholm C and Lee Y S 2016 *Phys. Rev. B* **94** 060409
- [43] Kelly Z A, Gallagher M J and McQueen T M 2016 *Phys. Rev. X* **6** 041007
- [44] Supplemental Material contains details on fitting of the Knight shift data, AC susceptibility at different frequencies, etc
- [45] Zaletel M P and Vishwanath A 2015 *Phys. Rev. Lett.* **114** 077201

Supplemental Material for “Gapped spin-1/2 spinon excitations in a new kagome quantum spin liquid compound $\text{Cu}_3\text{Zn}(\text{OH})_6\text{FBr}$ ”

1. Fitting of the Knight shift data

Here we discuss the fitting of the Knight shift data using different functions.

In Fig. S1, we employ a function form, $K_{\text{chem}} + A \exp(-\Delta/T)$, to fit the low temperature data and extract the size of the gap at different fields. The $K_{\text{chem}} = 0.015\%$ was obtained from the K - χ plot in the inset of Fig. 3(b) of the main text, and A is a free fitting parameter.

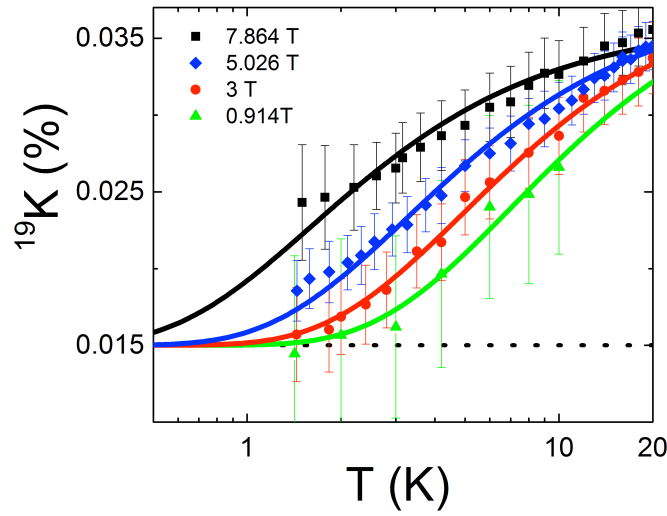


Fig. S1. Knight shift data fitted with $K_{\text{chem}} + A \exp(-\Delta/T)$.

In the main text, we do not include temperature prefactor in the fitting as in Ref. 29, $K_{\text{chem}} + AT \exp(-\Delta/T)$. The reason is following: Knight shift measures the density of states (DOS) which counts the number of low energy levels of excitations. Actually, antiferromagnetic correlations only affect the spectrum weight of the energy levels, but not the number of them. In others words, correlations will change the wave packet of quasi-particles, but do not annihilate or create them.

A trial of fitting our data with, $K_{\text{chem}} + AT \exp(-\Delta/T)$, shows that it cannot render a good fit. As shown in Fig. S2, the dashed lines cannot even go through the data points. Moreover, the obtained gap size becomes negative at large fields (can be seen in Tab. S1.), which is irrational. We hence argue, that if one wants to take antiferromagnetic correlations into account, a Currie-Weiss factor, $C/(T+\theta)$, should be used, namely, $K_{\text{chem}} + C/(T+\theta)\exp(-\Delta/T)$. The corresponding results are shown in Fig. S3 in which data points over a much wider temperature range fit to the function. The gap size obtained by using different fitting functions are summarized in the Tab. S1. The Δ obtained from a fitting to $K_{\text{chem}} + C/(T+\theta)\exp(-\Delta/T)$ is slightly larger than that obtained from the fitting to $K_{\text{chem}} + A \exp(-\Delta/T)$, but the magnetic field dependence of the gap size is the same, as can be in Fig. S4. To be more conservative on the estimate of the gap size, in the main text we use the fitting form,

$K_{\text{chem}} + A \exp(-\Delta/T)$, which gives a smaller Δ .

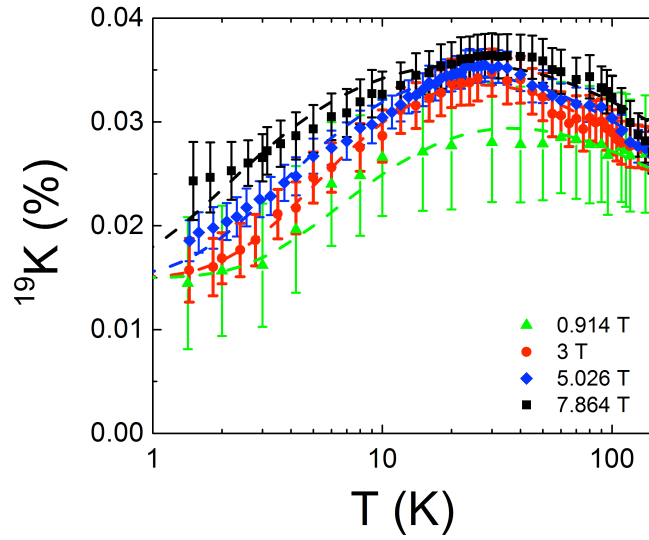


Fig. S2. Knight shift data fitted with $K_{\text{chem}} + AT \exp(-\Delta/T)$.

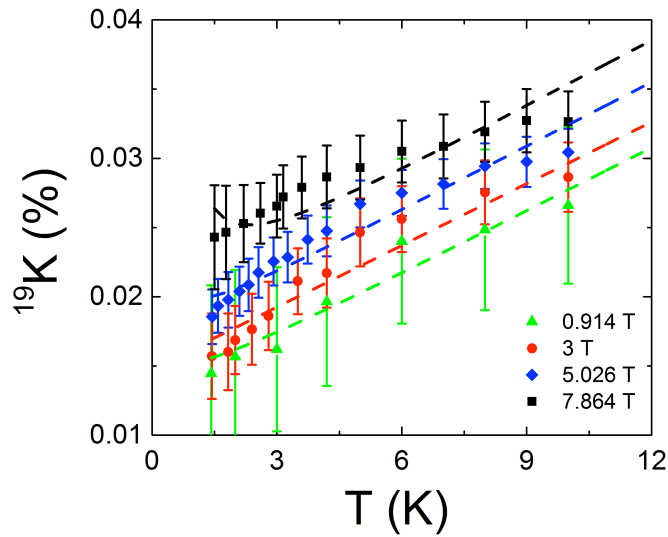


Fig. S3. Knight shift data fitted with $K_{\text{chem}} + C/(T+\theta) \exp(-\Delta/T)$.

H (T)	Δ obtained from different fitting functions	
	$K_{\text{chem}} + AT \exp(-\Delta/T)$	$K_{\text{chem}} + C/(T+\theta) \exp(-\Delta/T)$
0.914	1.90 ± 1.43	7.18 ± 0.41
3	0.15 ± 0.53	5.65 ± 0.23
5.026	-1.17 ± 0.21	3.81 ± 0.16
7.864	-2.32 ± 0.20	2.16 ± 0.16

Tab. S1. The gap value obtained from two different fitting schemes.

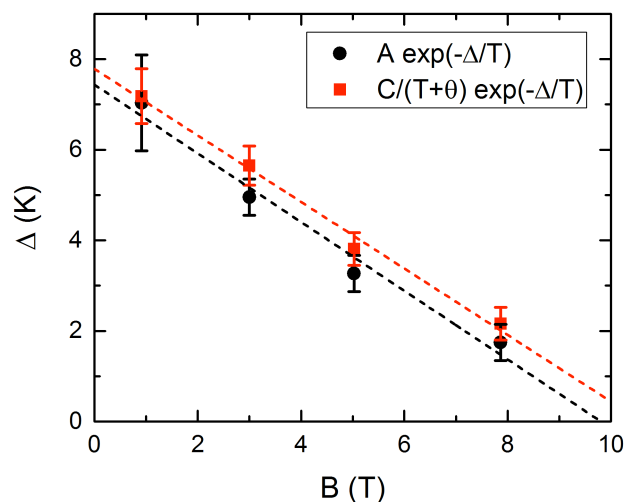


Fig. S4. Gap size obtained from two different fitting forms are consistent with each other.

2. Knight shift and magnetic susceptibility as a function of temperature

In Fig. S5, we compare the temperature dependence of macroscopic susceptibility data (red squares) and the Knight shift data (black circles) at magnetic field $B=3$ T. It is clearly seen that they scale one another at high temperatures of $T > 75$ K.

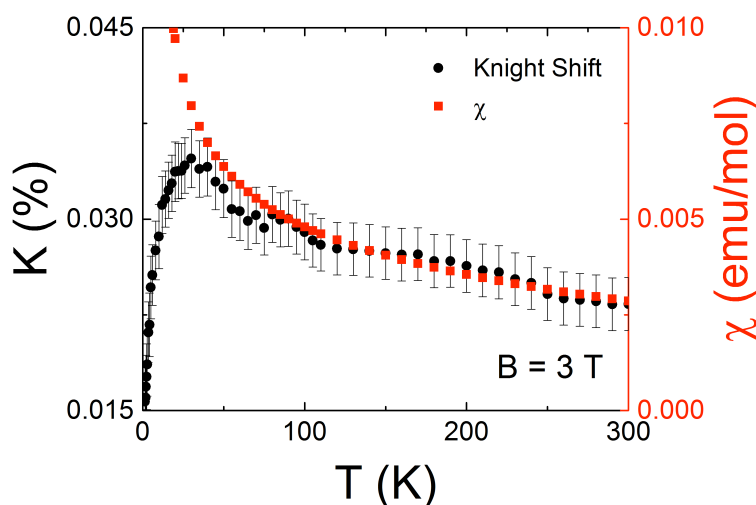


Fig. S5. Comparison of macroscopic susceptibility and the Knight shift data.

3. No contribution from free spins evidenced by spectra with different τ

In the Fig. 3 (a) of the main text, the spectra become slightly asymmetric and a bit wider at 55 K. To explore the possible reason behind this, we have performed further NMR measurements with different pulse interval (τ) at $T=55$ K and 4.2 K. The results are shown in Fig. S5 (a) and (b). The spectra become asymmetric at 55 K and this fact is attributed to magnetic anisotropy as mentioned in the main text. To confirm that the shoulder is not from free spins due to defect which should have a shorter spin-spin relaxation time T_2 , we compare the lineshape measured with

different τ . If there is contribution due to free spins due to defect or other magnetic impurities, the spectra will become sharper with longer τ , as in the work by M. Fu, T. Imai, T.-H. Han, Y.S. Lee, (Science 350 (2015) 655.) Fig. S4. However, our spectra do not become sharper when using longer τ , which proves that our spectra have no such contribution. The small increase of the shoulder with longer τ can be understood as due to an anisotropy of T_2 .

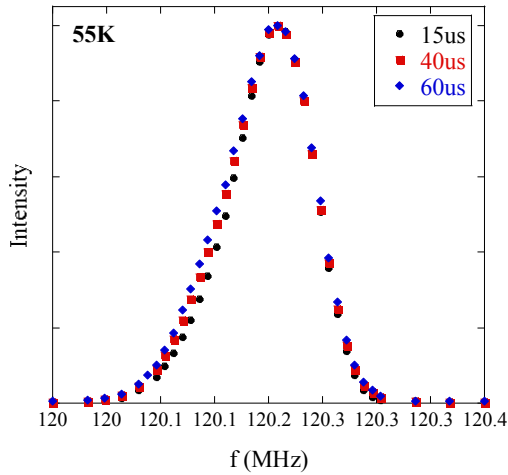


Fig. S6. (a) Spectra measured with different τ at 55K.

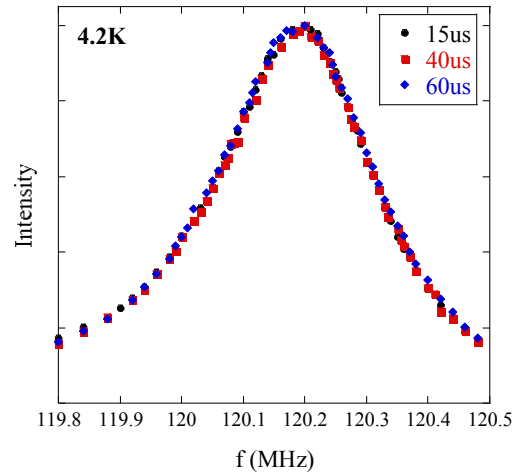


Fig. S6. (b) Spectra measured with different τ at 4.2K.

4. AC susceptibility at different frequencies

One may worry that the broadening of the NMR spectra at low temperatures could be caused by a formation of spin glass. To exclude the possibility of glassy behavior in our material, we have further performed magnetic susceptibility measurements at different frequencies. As shown in Fig. S7, at $B=1$ T and $B=5$ T, the temperature dependence of the magnetic susceptibility shows no frequency dependence, which safely rules out the possibility of spin glass behavior in our material.

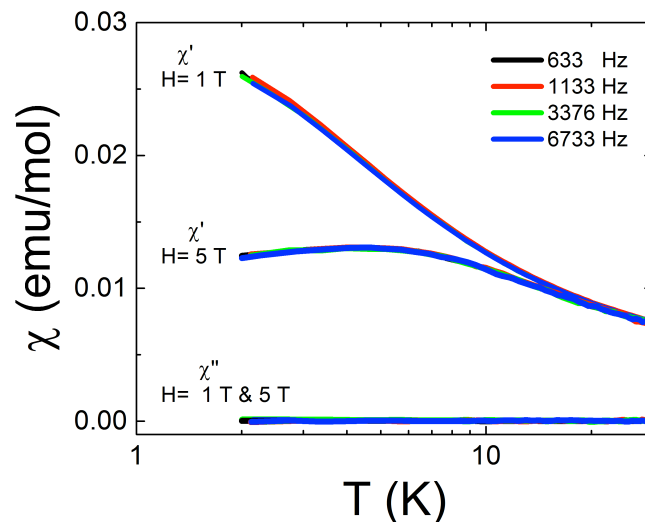


Fig. S7. Temperature dependence of the magnetic susceptibility at different magnetic fields and different frequencies. Clearly, no sign of spin glass type of slow dynamics can be seen.

Moreover, in Fig. S7, besides the real part of magnetic susceptibility χ' , we have also shown the imaginary part χ'' , and it is zero throughout, which also means there is no dissipation of our system due to spin glass or other mechanism.